

# A High-Isolation Sub-6 GHz In-Band Full-Duplex Communication System

Chengzhe Shi\*, Wensheng Pan\*, Wanzhi Ma\*, Ying Liu\*, Qiang Xu\*, Zhiya Zhang<sup>†</sup> and Shihai Shao\*

\*National Key Laboratory of Wireless Communications,

University of Electronic Science and Technology of China, Chengdu, P. R. China

Email: scz@std.uestc.edu.cn, panwens@uestc.edu.cn, mawanzhi@uestc.edu.cn,

yliu85@uestc.edu.cn, xuqiang06@uestc.edu.cn, ssh@uestc.edu.cn

<sup>†</sup> Xidian university, Xi'an 710071, P. R. China

E-mail: zyzhang@xidian.edu.cn

**Abstract**—In 5G networks, the sub-6 GHz band offers broader user coverage and more reliable connections compared to its millimeter-wave counterpart. The increasing spectrum congestion in sub-6 GHz has driven research into the in-band full-duplex (IBFD) communication. This work explores the design principles of a high-isolation IBFD transceiver prototype for future 5G-Advanced networks. The designed IBFD transceiver employs a high-isolation spiral antenna design, which offers high spatial isolation while avoiding the complicated radio frequency self-interference cancellation. Prototype test results demonstrate that the provided spatial isolation is over 70 dB, and the overall self-interference cancellation performance exceeds 120 dB combined with nonlinear digital self-interference cancellation.

## I. INTRODUCTION

In 5G networks, the sub-6 GHz frequency band (ranging from 600 MHz to 6 GHz) is highly regarded due to its balanced attributes of coverage and capacity. Compared to the millimeter-wave (mmWave) band, the sub-6 GHz band offers a broader coverage range and superior penetration through buildings and vegetation, thus ensuring reliable connectivity in urban, suburban, and rural environments [1], [2].

Currently, the sub-6 GHz band is not only favored by mobile network operators but also widely used by other wireless services such as Wi-Fi, satellite communications, and military applications. This intense competition for spectrum resources may lead to congestion and limit the potential of 5G networks to fully exploit this band [3]. To facilitate flexible use of radio resources, 3GPP Release 18, the initial release of 5G-Advanced, included a study item on the feasibility of simultaneous uplink and downlink in the same frequency band, also known as in-band full-duplex (IBFD) [4]. Potential IBFD features are anticipated to be incorporated into the specifications from Release 19 onward. Recently, the 3rd Generation Partnership Project (3GPP) completed the study of subband full-duplex, which may pave the way for commercial deployments of IBFD in 5G-Advanced and 6G.

IBFD technology allows simultaneous transmission and reception on the same frequency channel, theoretically doubling spectral efficiency compared to traditional half-duplex mode, making it a crucial technology to meet the high data rate demands of 5G and 5G-Advanced [5], [6]. However, achieving

full duplex communication presents significant technical challenges, primarily related to self-interference (SI), where the transmitter interferes with its own receiver. Overcoming these challenges requires advances in self-interference cancellation (SIC) techniques, typically involving three-stage cancellation in the spatial, RF, and digital domains [6]. The successful integration of these cancellation techniques is crucial for the development of high-performance IBFD transceiver systems.

Recently, a mmWave full-duplex prototype testing platform, developed in accordance with 5G Integrated Access and Backhaul (IAB) specifications, demonstrated the feasibility of a mmWave SIC transceiver [7]. Experimental results confirmed that full-duplex throughput in IAB scenarios could potentially double compared to half-duplex systems. By leveraging the high path loss of the mmWave frequency band and a passive antenna design with multiple isolators, spatial isolation exceeding 80 dB was achieved.

As a complementary frequency band to mmWave in 5G networks, the sub-6 GHz band lacks the advantage of high path loss and available spatial degrees of freedom. Consequently, designing high-isolation IBFD transceiver prototypes in the sub-6 GHz band is essential for 5G deployment. In this work, we investigate the design principles of SIC for IBFD systems for the sub-6 GHz band, and a full-duplex prototype with high-isolation spiral antennas is designed, which provides high spatial isolation without the complicated radio frequency (RF) SIC designs. Prototype testing results demonstrate the spatial SI isolation of over 70 dB, and the overall SIC capability exceeding 120 dB combined with nonlinear digital SIC (DSIC).

## II. HIGH-ISOLATION IBFD TRANSCEIVER DESIGN PRINCIPLES

The coupling between transmit and receive antennas in IBFD radios results in significant SI at the receiver, overshadowing the desired signal from remote uplink users. Therefore, a primary challenge in implementing IBFD radios is to cancel the SI to the level of background noise. For instance, 5G base stations typically operate with an effective isotropic radiated power (EIRP) of 40 to 50 dBm. At such a transmit power level, the overall required SIC capability to cancel SI to noise

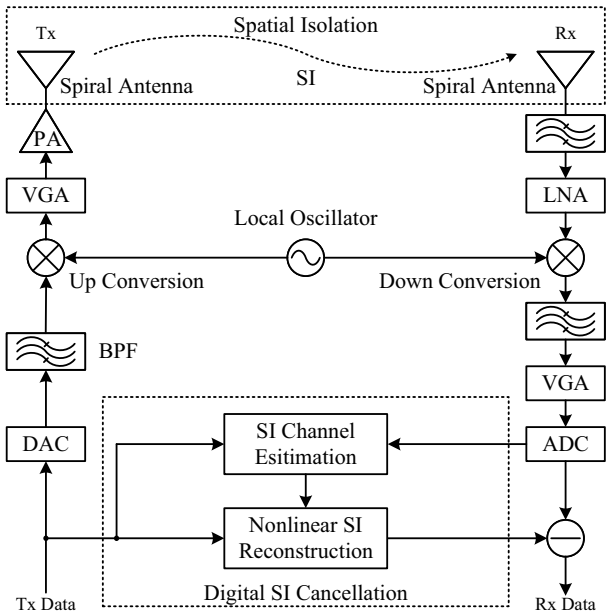


Fig. 1. Schematic diagram of the high-isolation IBFD SIC transceiver.

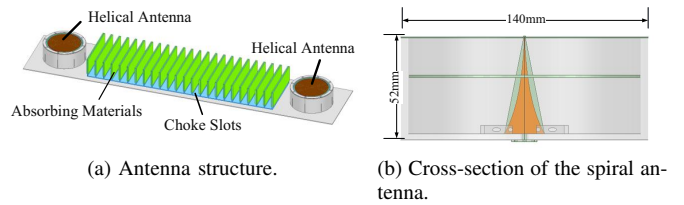


Fig. 2. High-isolation wideband spiral antennas. (a) Antenna structure. (b) Cross-section of the spiral antenna.

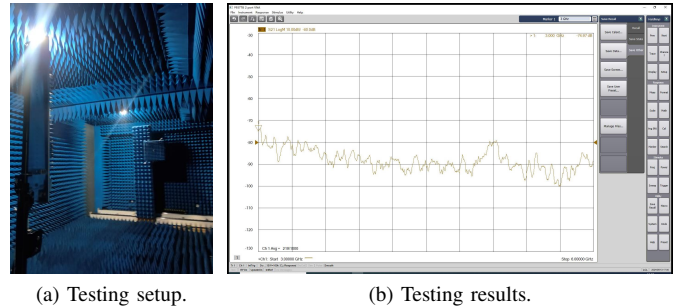


Fig. 3. The anechoic chamber testing setup and results for the high-isolation spiral antenna. (a) Testing setup. (b) Testing results.

floor could be as high as 129 dB given -79 dBm noise floor at 300 MHz bandwidth with 10 dB noise figure.

Given such strong SI, it is necessary to implement cancellation in both the spatial domain and the receive RF front-end to reduce SI; otherwise, it would severely saturate the receiver. Typically, the saturation power of the receive RF front-end, determined by the low noise amplifier (LNA), is in the range of -20 to -10 dBm, which implies that the spatial domain and RF front-end must be able to mitigate more than 70 dB of SI.

Moreover, transmit error vector magnitude (EVM) distortion resulting from impairments in the transmit chain also degrades the performance of IBFD radios. For instance, in 5G networks, typical transmit powers are 20 dBm for user equipment and 46 dBm for base stations. Hence, a 17.5% transmit EVM distortion in the base station exceeds the transmit power of user equipment by an order of magnitude<sup>1</sup> [8]. Considering the path loss, the signal received at the base station from user equipment is much weaker than the EVM distortion introduced by the base station transmitter, necessitating the DSIC.

Taking into account the SIC requirements outlined above, we design a SIC transceiver for IBFD, as shown in Fig 1. Our IBFD prototype design employs joint spatial and digital SIC schemes. The complex RF SIC has been omitted due to the high isolation provided by the circular polarized spiral antenna design, which ensures that the receive RF front-end does not saturate due to strong SI, thus preserving sufficient dynamic range for the analog-to-digital converter (ADC) to capture the desired signal. Furthermore, through nonlinear DSIC, we anticipate reducing the residual SI after ADC sampling, dominated by distortions in the transmit chain, to the noise floor level.

<sup>1</sup>In 5G, the maximum allowed EVM levels for base station transmitters are 17.5% for QPSK, corresponding to -15 dB power levels for the distortion of the transmitted signal.

### A. High Isolation spiral Antenna

In IBFD systems, the SI arising from the transmit antenna coupling to the receive antenna poses a significant risk of saturating the receive RF front-end, particularly in the sub-6 GHz band where spatial attenuation is relatively low. Specifically, these mutual coupling effects can be categorized into surface and space wave coupling. The latter can be subdivided into direct radiation coupling (line-of-sight component) and space reflection coupling (reflection component) [6]. In high-density array systems, the high spatial degrees of freedom can be leveraged to employ active beamforming SIC techniques to mitigate near-field coupling between transmit and receive arrays [9]–[11]. However, in sub-6 GHz, the limited spatial degrees of freedom make it crucial to enhance the spatial isolation through specialized antenna design.

In our IBFD prototype design, we adopt a solution involving high-isolation wideband spiral antennas, as depicted in Fig 2. The high-isolation wideband spiral antennas comprise two co-polarized spiral antenna elements, choke slots, and absorbing materials.

A spiral antenna is constructed from a helix-shaped metallic conductor, typically made from wire or tubing. It is commonly fed with a coaxial cable, where the inner conductor connects to one end of the helix and the outer conductor is grounded to a metal plate. This ground plate diminishes induced currents on the coaxial cable's surface, enhancing the antenna's radiation characteristics and minimizing backward radiation.

As shown in Fig 2 (a), a choke slot structure is integrated between the two antenna elements, providing several advantages. Firstly, unlike a smooth metal ground plate, the metal plate with choke slots directly impedes surface wave propagation, effectively reducing coupling between the transmit and receive antennas. Secondly, since the height of the choke slots is higher

than that of the spiral antennas, they can significantly suppress the direct radiation coupling of electromagnetic waves. Moreover, absorbing materials are applied onto the dielectric floor and the surface of the choke slots, which absorb space-reflected waves, further reducing electromagnetic interference between antenna elements.

Fig 3 (a) illustrates the anechoic chamber testing setup for the high-isolation spiral antenna. The S21 parameter, which characterizes the isolation, is also depicted in Fig 3 (b). It can be seen that within the 3~6 GHz testing frequency range, the antenna isolation is generally above 80 dB, with a slight degradation between 3~3.5 GHz, indicating overall good isolation performance.

### B. Without RF SIC

Typically, the RF SIC is an effective method to prevent saturation or blocking of the receive RF front-end caused by SI, although it necessitates additional complex circuitry for implementation. Benefiting from the design of the high-isolation spiral antenna, spatially coupled SI is effectively suppressed, greatly avoiding the risk of RF front-end saturation. This also ensures that ADCs have sufficient dynamic range to sample both SI and the desired signal simultaneously. As a result, our IBFD prototype design obviates the complex RF SIC.

### C. Nonlinear Digital SIC

In practical engineering, constrained by hardware complexity and cost, merely reducing SI through spatial isolation and RF cancellation is insufficient. The residual SI after ADC sampling still contaminates the desired signal, resulting in decreased receive sensitivity. Therefore, it is necessary to further cancel the residual SI in the digital domain to reach the demodulation threshold of the desired signal.

After upconverting the baseband signal to the RF domain, inevitable nonlinear interference components arise, induced by factors such as phase noise, I/Q imbalance, and power amplifier (PA) nonlinearities. As transmit power increases, the impact of PA-dominated nonlinear interference becomes more pronounced. Let  $x(n)$  denote the digital baseband signal. Considering the PA's nonlinear distortion characteristics and memory effects, the discrete form of the transmitted signal can be expressed according to the widely used memory polynomial (MP) model as

$$\begin{aligned} x_T(n) &= f_{\text{MP}}[x(n)] + z_T(n) \\ &= \sum_{p=0}^{P-1} \sum_{m=0}^{M-1} \alpha_{mp} \phi_{m,p}[x(n)] + z_T(n), \end{aligned} \quad (1)$$

where  $f_{\text{MP}}[\cdot]$  represents the nonlinear MP function,  $P$  denotes the maximum order of nonlinearity,  $M$  is the maximum memory depth, and  $\phi_{m,p}[\cdot]$  is the MP basis function with respect to the nonlinear order  $p$  and memory depth  $m$ , which is given by

$$\phi_{m,p}[x(n)] = x(n-m) |x(n-m)|^{2p}, \quad (2)$$

and  $\alpha_{mp}$  is the corresponding coefficient.

After propagating through a multipath channel, the digital model of the SI received by the local antenna is

$$\begin{aligned} y(n) &= h_{\text{SI}}(n) \otimes f_{\text{MP}}[x(n)] + z_{\text{R}}(n) \\ &= \sum_{i=1}^L h_i f_{\text{MP}}[x(n - D_i)] + z_{\text{R}}(n) \\ &= \sum_{i=1}^L h_i \sum_{p=0}^{P-1} \sum_{m=D_{I,i}}^{M+D_{I,i}-1} \alpha_{mp} \phi_{m+D_{F,i,p}}[x(n)] + z_{\text{R}}(n), \end{aligned} \quad (3)$$

where  $z_{\text{R}}(n)$  represents the receive noise,  $h_i$  is the complex gain of the  $i$ -th path, and  $D_i = D_{I,i} + D_{F,i}$  is the normalized delay (with respects to the sampling time) of the  $i$ -th path, including an integer part  $D_{I,i}$  and a fractional part  $D_{F,i}$ .

Since  $\phi_{m+D_{F,i,p}}[x(n)]$  is the signal  $\phi_{m,p}[x(n)]$  delayed by a fractional delay  $D_{F,i}$ , it can be modeled with an ideal fractional delay filter as

$$\begin{aligned} \phi_{m+D_{F,i,p}}[x(n)] &= \phi_{m,p}[x(n)] \otimes h_{D_{F,i}}(n) \\ &= \sum_{j=-K}^{+K} h_{D_{F,i}}(j) \phi_{m+j,p}[x(n)], \end{aligned} \quad (4)$$

where  $h_{D_{F,i}}(n) = \text{sinc}(n - D_{F,i})$  is the impulse response of the ideal fractional delay filter. Moreover, the filter coefficients are truncated from  $-K$  to  $K$  by a rectangular window to meet practical engineering requirements.

After nonlinear distortion and multipath channel propagation, the received SI comprises linear and nonlinear components, alongside noise, which is omitted in the subsequent derivation for convenience. The received SI can be expressed in polynomial form

$$\begin{aligned} y(n) &= \sum_{i=1}^L \sum_{j=-K}^K \sum_{p=0}^{P-1} \sum_{m=D_{I,i}}^{M+D_{I,i}-1} \beta_{ijmp} \phi_{m+j,p}[x(n)] \\ &= \sum_{i=1}^L \sum_{k=m-K}^{m+K} \sum_{p=0}^{P-1} \sum_{m=D_{I,i}}^{M+D_{I,i}-1} \beta_{ikmp} \phi_{k,p}[x(n)], \end{aligned} \quad (5)$$

where  $\beta_{ijmp} = h_i \alpha_{mp} h_{D_{F,i}}(j)$  and  $\beta_{ikmp} = h_i \alpha_{mp} h_{D_{F,i}}(k - m)$ . To further simplify (5), the following transformation is performed

$$\begin{aligned} y(n) &= \sum_{i=1}^L \sum_{k=-K+D_{I,i}}^{K+D_{I,i}+M-1} \sum_{p=0}^{P-1} \sum_{m=D_{I,i}}^{M+D_{I,i}-1} \beta'_{ikmp} \phi_{k,p}[x(n)] \\ &= \sum_{i=1}^L \sum_{k=-K+D_{I,\min}}^{K+D_{I,\max}+M-1} \sum_{p=0}^{P-1} \sum_{m=D_{I,i}}^{M+D_{I,i}-1} \beta''_{ikmp} \phi_{k,p}[x(n)] \\ &= \sum_{k=-K+D_{I,\min}}^{K+D_{I,\max}+M-1} \sum_{p=0}^{P-1} w_{k,p} \phi_{k,p}[x(n)], \end{aligned} \quad (6)$$

where

$$\beta'_{ipmk} = h_i \alpha_{mp} h'_{D_{F,i}}(k - m), \quad (7)$$

$$\beta''_{ipmk} = h_i \alpha_{mp} h''_{D_{F,i}}(k - m), \quad (8)$$

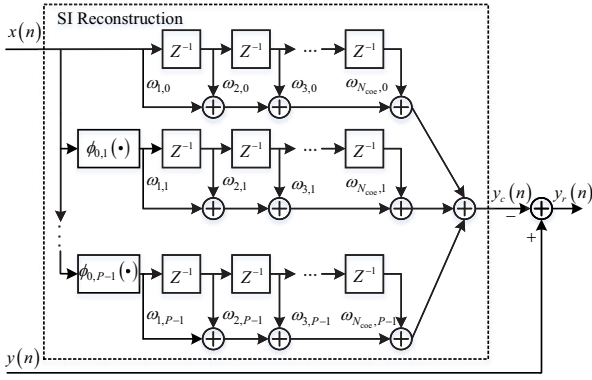


Fig. 4. Nonlinear DSIC adaptive filter structure.

$$h'_{D_{F,i}}(k-m) = \begin{cases} h_{D_{F,i}}(k-m), & -K \leq k-m \leq K \\ 0, & \text{otherwise} \end{cases}, \quad (9)$$

$$h''_{D_{F,i}}(k-m) = \begin{cases} h'_{D_{F,i}}(k-m), & -K + D_{I,i} \leq k \leq K + M + D_{I,i} - 1 \\ 0, & \text{otherwise} \end{cases}, \quad (10)$$

$D_{I,\max} = \max_i D_{I,i}$  and  $D_{I,\min} = \min_i D_{I,i}$  represent the maximum and minimum normalized arrival times of the SI after multipath channel propagation, respectively.  $w_{k,p}$  is the simplified basis function coefficients, which is given by

$$w_{k,p} = \sum_{i=1}^L \sum_{m=D_{I,i}}^{M+D_{I,i}-1} h_i \alpha_{mp} h''_{D_{F,i}}(k-m) \quad (11)$$

Assuming there are  $N$  sampling points, (6) can be expressed in matrix form as

$$\mathbf{Y} = \mathbf{X}\mathbf{w}, \quad (12)$$

where

$$\mathbf{Y} = [y(1), y(2), \dots, y(N)]^T, \quad (13)$$

$$\mathbf{X} = [\mathbf{X}_1, \mathbf{X}_2, \dots, \mathbf{X}_N]^T, \quad (14)$$

$$\mathbf{w} = \{w_{-K+D_{I,\min},0}, \dots, w_{K+M+D_{I,\min}-1,0}, \dots, w_{K+M+D_{I,\min}-1,P-1}\}^T, \quad (15)$$

$$\mathbf{X}_n = \{\phi_{-K+D_{I,\min},0}[x(n)], \dots, \phi_{K+M+D_{I,\min}-1,0}[x(n)], \dots, \phi_{K+M+D_{I,\min}-1,P-1}[x(n)]\}^T. \quad (16)$$

The optimal coefficient estimation with the least squares criterion can be expressed as

$$\hat{\mathbf{w}} = (\mathbf{X}^H \mathbf{X})^{-1} \mathbf{X}^H \mathbf{Y}. \quad (17)$$

As shown in Fig. 4, the nonlinear DSIC structure can be realized by configuring  $P$  one-dimensional adaptive filters in parallel, where each dimension has  $N_{\text{coe}}$  coefficients. Specifically, when the transmit power is relatively low, and the nonlinearity can be ignored, i.e.,  $P = 0$ , this structure can be simplified to a one-dimensional horizontal filter.

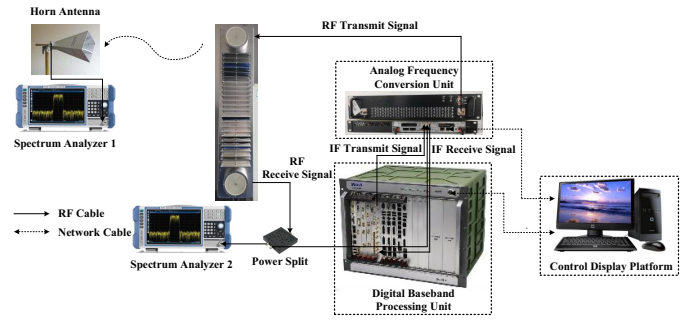


Fig. 5. Connection Diagram of the High-Isolation IBFD System.

Particularly, based on (6), the minimum number of taps for the adaptive filter structure can be derived as

$$N_{\min} = P(2K + M + \Delta D_I), \quad (18)$$

where  $\Delta D_I = D_{I,\max} - D_{I,\min}$  denotes the maximum delay spread of the SI channel. It can be seen that the minimum number of taps depends on the nonlinearity order  $P$ , the memory depth  $M$ , the window length  $K$  of the fractional delay filter, and the maximum delay spread  $\Delta D_I$ . However, it is independent of the number of multipaths  $L$ .

### III. HIGH-ISOLATION IBFD PROTOTYPING

The high-isolation IBFD system comprises a digital baseband processing unit (responsible for generating and receiving baseband signals, and implementing nonlinear DSIC), an analog frequency conversion unit (used for up-conversion and down-conversion of analog signals), the high-isolation spiral antennas and control display platform, as shown in Fig. 5.

#### A. Analog Frequency Conversion Unit

The transmit chain employs a combination of up-conversion and down-conversion schemes. An intermediate frequency (IF) signal with a center frequency of 300 MHz and a bandwidth of 300 MHz is first up-converted to 13 GHz. Subsequently, this signal is then down-converted to 1~6 GHz, resulting in a transmitted signal with center frequencies ranging from 1.15 GHz to 5.85 GHz.

Both receive chains also utilize a combination of up-conversion and down-conversion schemes. The received IF signal within the 1~6 GHz is first up-converted to 13 GHz, and then down-converted to a received signal with a center frequency of 300 MHz.

Importantly, both the transmit and receive chains use the same local oscillator to reduce the frequency offset and phase noise of SI.

#### B. Digital Baseband Processing Unit

The digital baseband processing unit generates the transmitted IF signal, receives the IF signal, executes the nonlinear DSIC algorithm, and outputs the signal after DSIC. Moreover, it also controls various modules via the serial peripheral interface (SPI). This unit includes one FPGA, six ADC channels, three DAC channels, one input 100 MHz reference clock, two

Ethernet ports, and five SPI control interfaces. The ADC channels are used to sample wideband signals with a bandwidth of 300 MHz and an IF of 300 MHz. The FPGA performs the nonlinear DSIC algorithm. The DAC channels are utilized to output the IF analog signal with a bandwidth of 300 MHz and an IF of 300 MHz.

The bandwidth signal generated by the baseband unit is formed by a Chu sequence, which has the advantages of constant envelope, zero cyclic autocorrelation, and low peak-to-average power ratio. When synchronizing with the received signal, a distinct correlation peak can easily be found by performing a sliding correlation between the locally stored known transmitted signal and the received signal. The Chu sequence is expressed as

$$x(n) = \begin{cases} \exp\left\{\frac{j\pi\mu[n(n+1)+2qn]}{N}\right\}, & N \text{ is odd} \\ \exp\left\{\frac{j\pi\mu(n^2+2qn)}{N}\right\}, & N \text{ is even} \end{cases}, \quad (19)$$

where  $\mu \in \{1, 2, \dots, N-1\}$ , and  $q$  is any integer.

Specifically, the baseband unit uses Chu sequences with  $\mu = 1$  and  $q = 0$ , assembled into a 2048-point OFDM signal for transmission. The bandwidth of the OFDM signal is 300 MHz with a sampling rate of 245 MSPS. The number of effective subcarriers is  $\frac{200 \times 2048}{245} \approx 1672$ , which is the length of the Chu sequence. The length of the OFDM pilot sequence is 72, making the total length of one OFDM signal 2120. After 4x upsampling, the OFDM signal with a sampling rate of 980 MSPS is converted from serial to parallel, resulting in four 245 MSPS signals, which are then upconverted and output by the DAC.

#### IV. PROTOTYPE TEST

##### A. Test Environment

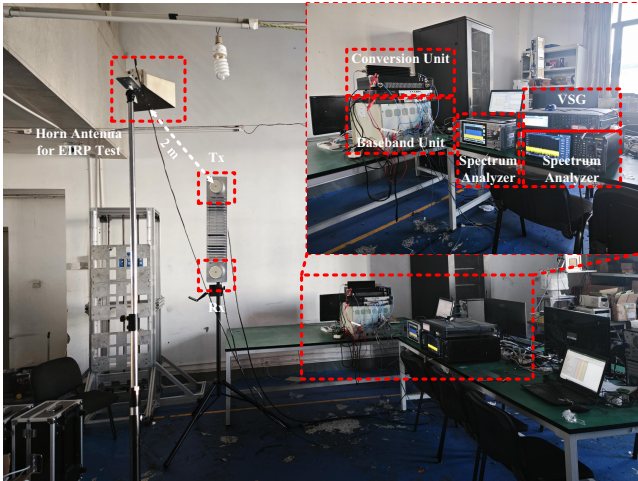


Fig. 6. High-Isolation IBFD Prototype Testing Scenario.

The testing process is conducted in a typical laboratory environment, as shown in Fig. 6. The baseband signal is

transformed into a 300 MHz analog signal through the digital baseband processing unit and sent to the frequency conversion unit. This IF analog signal then undergoes a two-stage up-conversion process to achieve the desired RF frequency range of 1~6 GHz. Subsequently, the signal is transmitted through the spiral antenna. The receive antenna captures the SI and outputs it after spatial isolation. The output signal is split into two paths by a power splitter. One path is sent to the spectrum analyzer to observe the interference power after spatial isolation, and the other path is fed into the DSIC unit, which can be enabled or disabled. After DSIC, the processed output is displayed on a control display interface.

Auxiliary equipment required for the experimental testing includes a vector signal generator (VSG) to calibrate the receive chain gain. A receive horn antenna is placed 2 meters away from the experimental system to receive the transmitted signal for EIRP testing. All auxiliary equipment is connected to a switch via Ethernet cables to facilitate centralized control.

##### B. Metric Definition and Test Method

The SIC test procedure for the high-isolation IBFD prototype is as follows:

- 1) Connect the test equipment as depicted in Fig. 5, load the transmission waveform, and set the operating center frequency of the prototype  $f_c$  to 3.15 GHz.
- 2) Set the integration bandwidth of all spectrum analyzers to 300 MHz.
- 3) Measure the power of spectrum analyzer 1, denoted as  $P_{\text{meas}}$ , and calculate the EIRP:

$$\text{EIRP (dB)} = P_{\text{meas}} + L_{\text{path}} + L_{\text{cable}} - G_{\text{horn}} + 3, \quad (20)$$

where  $L_{\text{cable}}$  is the cable loss from the horn antenna to the spectrum analyzer,  $G_{\text{horn}}$  is the gain of the horn antenna, and  $L_{\text{path}} = 20 \lg D \text{ (km)} + 20 \lg f_c \text{ (MHz)} + 32.5$  is the free-space loss between the transmit spiral antenna and the horn antenna with a distance of 2 meters. Moreover, 3 dB is attributed to the polarization loss, where the transmit antenna exhibits circular polarization and the receive antenna is linear polarization.

- 4) Measure the power of spectrum analyzer 2, denoted as  $P_{\text{r1}}$ , and the air interface equivalent residual SI power is  $I_{\text{air}} \text{ (dBm)} = P_{\text{r1}} - G_{\text{r1}}$ , where  $G_{\text{r1}}$  represents the receiver front-end gain (mainly including the antenna, cables, and power dividers).
- 5) Calculate the spatial isolation  $\text{ISO (dB)} = \text{EIRP} - I_{\text{air}}$ .
- 6) Enable the DSIC unit and record the received power after DSIC as  $P_{\text{r2}}$ . Then, the air interface equivalent residual SI power after DSIC is  $I_{\text{res}} \text{ (dBm)} = P_{\text{r2}} - G_{\text{r2}}$ , where  $G_{\text{r2}}$  represents the total receive gain (mainly including the frequency conversion unit and the digital baseband unit).
- 7) Calculate the DSIC capability  $\text{SIC}_{\text{digital}} \text{ (dB)} = I_{\text{air}} - I_{\text{res}}$ .
- 8) Calculate the overall SIC capability of the prototype  $\text{SIC}_{\text{total}} \text{ (dB)} = \text{EIRP} - I_{\text{res}} = \text{ISO} + \text{SIC}_{\text{digital}}$ .

TABLE I

THE TEST RESULTS OF THE HIGH-ISOLATION FULL-DUPLEX PROTOTYPE.

Parameter	Vaule			
Center Frequency (GHz)	3.15	4	5	5.85
Bandwidth (MHz)	300	300	300	300
Receive power of spectrum analyzer 1 (dBm)	2.9	-1.0	-6.6	-2.0
Horn antenna gain (dB)	5.2	9.5	10.5	12.3
Cable loss (dB)	3.9	4.7	5.9	6.7
Path loss (dB)	48.4	50.5	52.4	53.8
EIRP (dBm)	53.2	47.7	44.2	49.1
SI Power before DSIC (dBm)	-24.0	-23.2	-26.1	-24.9
Spatial isolation (dB)	77.2	70.9	70.3	74.0
SI Power after DSIC (dBm)	-77.4	-77.8	-76.5	-78.3
DSIC capability (dB)	53.3	54.6	50.4	53.4
Prototype SIC capability(dB)	130.5	125.5	120.7	127.4

9) Change the operating frequencies to 4 GHz, 5 GHz, and 5.85 GHz, and repeat steps (3) through (8) to complete performance testing at different center frequencies.

### C. Test Results

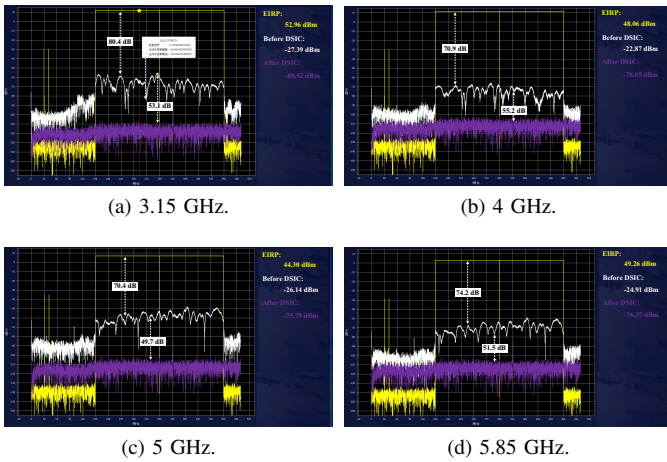


Fig. 7. The power spectral density of SIC at each stage for different center frequencies shown on the control display interface. (a) 3.15 GHz. (b) 4 GHz. (c) 5 GHz. (d) 5.85 GHz.

Fig.7 shows the power spectral density of SIC at each stage on the control display interface, where the yellow solid line represents the transmitted EIRP, and the white and purple solid lines represent the SI before and after DSIC, respectively. It can be observed that the SI after spatial isolation exhibits significant in-band frequency selectivity. This implies that RF SIC would require numerous analog taps and delay lines with wide tunability, thereby increasing the complexity of practical implementation.

However, due to the high-isolation design of the spiral antenna, our IBFD prototype obviates the requirement for complex RF SIC circuits. The measured spatial isolation of the designed spiral antenna structure is approximately 70~80 dB, which is slightly lower than the anechoic chamber test results, possibly due to the rich indoor reflection components. Furthermore, by combining the nonlinear DSIC algorithm, a digital cancellation performance of over 50 dB has been

achieved, reducing the residual SI power to near the noise floor level (approximately -79 dBm). The detailed test results of the prototype across different frequency bands from 3 to 6 GHz are provided in Table I. According to the test results, the designed prototype demonstrates an overall SIC capability exceeding 120 dB across all tested frequency bands.

### V. CONCLUSION

In this work, we explore the design principles of SIC for IBFD systems in the sub-6 GHz band and develop a high-isolation IBFD prototype for future 5G-Advanced networks. The designed IBFD prototype employs a high-isolation spiral antenna design, which provides substantial spatial isolation without the need for complex RF SIC design. Prototype test results indicate that the provided spatial isolation is over 70 dB, and the overall SIC performance exceeds 120 dB combined with the nonlinear DSIC.

### ACKNOWLEDGMENT

This work was supported in part by the National Natural Science Foundation of China under Grant 62071094, and Grant 61901396, and the National Key Laboratory of Wireless Communications Foundation under Grant 6142102222504.

### REFERENCES

- [1] Y. Huang and Y. Huang, "Challenges and opportunities of sub-6 ghz integrated sensing and communications for 5g-advanced and beyond," *Chinese Journal of Electronics*, vol. 33, no. 2, pp. 323–325, 2024.
- [2] S.-M. Kim, J. Kim, H. Cha, M. S. Sim, J. Choi, S.-W. Ko, C.-B. Chae, and S.-L. Kim, "Opportunism in spectrum sharing for beyond 5g with sub-6 ghz: A concept and its application to duplexing," *IEEE Access*, vol. 8, pp. 148 877–148 891, 2020.
- [3] B. Smida, R. Wichman, K. E. Kolodziej, H. A. Suraweera, T. Riihonen, and A. Sabharwal, "In-band full-duplex: The physical layer," *Proceedings of the IEEE*, 2024.
- [4] 3GPP, "Study on evolution of nr duplex operation," *Technical Specification 38.858, 3rd Generation Partnership Project (3GPP)*, 2023.
- [5] M. Duarte, C. Dick, and A. Sabharwal, "Experiment-driven characterization of full-duplex wireless systems," *IEEE Transactions on Wireless Communications*, vol. 11, no. 12, pp. 4296–4307, 2012.
- [6] K. E. Kolodziej, B. T. Perry, and J. S. Herd, "In-band full-duplex technology: Techniques and systems survey," *IEEE Transactions on Microwave Theory and Techniques*, vol. 67, no. 7, pp. 3025–3041, 2019.
- [7] B. Yu, C. Qian, J. Lee, S. Shao, Y. Shen, W. Pan, P. Lin, Z. Zhang, J. Jung, S. Choi *et al.*, "Realizing high power millimeter wave full duplex: Practical design, prototype and results," in *GLOBECOM 2022-2022 IEEE Global Communications Conference*. IEEE, 2022, pp. 3803–3808.
- [8] 3GPP, "Evolved universal terrestrial radio access (e-utra); base station (bs) radio transmission and reception," *Technical Specification 36.104, 3rd Generation Partnership Project (3GPP)*, vol. 10, 2023.
- [9] I. P. Roberts and S. Vishwanath, "Beamforming cancellation design for millimeter-wave full-duplex," in *2019 IEEE Global Communications Conference (GLOBECOM)*. IEEE, 2019, pp. 1–6.
- [10] C. Shi, W. Pan, Y. Shen, and S. Shao, "Robust transmit beamforming for self-interference cancellation in star phased array systems," *IEEE Signal Processing Letters*, vol. 29, pp. 2622–2626, 2022.
- [11] X. Huang, A. T. Le, and Y. J. Guo, "Transmit beamforming for communication and self-interference cancellation in full duplex mimo systems: A trade-off analysis," *IEEE Transactions on Wireless Communications*, vol. 20, no. 6, pp. 3760–3769, 2021.